JQS Journal of Quaternary Science

QRA
Quaternary Research Association

Elaia, Pergamon's maritime satellite: the rise and fall of an ancient harbour city shaped by shoreline migration

MARTIN SEELIGER,[1]* ANNA PINT,[2] STEFAN FEUSER,[3] SVENJA RIEDESEL,[4] NICK MARRINER,[5] PETER FRENZEL,[6] FELIX PIRSON,[7] ANDREAS BOLTEN[2] and HELMUT BRÜCKNER[2]

[1]Department of Physical Geography, Faculty of Geosciences, Goethe-University Frankfurt, Germany
[2]Institute of Geography, University of Cologne, Germany
[3]Institute of Classical Studies, Kiel University, Germany
[4]Department of Geography and Earth Sciences, Aberystwyth University, UK
[5]CNRS, Laboratoire Chrono-Environnement UMR6249, Université de Bourgogne-Franche-Comté, France
[6]Institute of Earth Sciences, Friedrich Schiller University of Jena, Germany
[7]German Archaeological Institute (DAI), Istanbul, Turkey

ABSTRACT: Throughout human history, communication and trade have been key to society. Because maritime trade facilitated the rapid transportation of passengers and freight at relatively low cost, harbours became hubs for traffic, trade and exchange. This general statement holds true for the Pergamenian kingdom, which ruled wide parts of today's western Turkey during Hellenistic times. Its harbour, located at the city of Elaia on the eastern Aegean shore, was used extensively for commercial and military purposes. This study reconstructs the coastal evolution in and around the ancient harbour of Elaia and compares the observed environmental modifications with archaeological and historical findings. We use micropalaeontological, sedimentological and geochemical proxies to reconstruct the palaeoenvironmental dynamics and evolution of the ancient harbour. The geoarchaeological results confirm the archaeological and historical evidence for Elaia's primacy during Hellenistic and early Roman times, and the city's gradual decline during the late Roman period. Furthermore, our study demonstrates that Elaia holds a unique position as a harbour city during ancient times in the eastern Aegean region, because it was not greatly influenced by the high sediment supply associated with river deltas. Consequently, no dredging of the harbour basins is documented, creating exceptional geo-bioarchives for palaeoenvironmental reconstructions. Copyright © 2019 John Wiley & Sons, Ltd.

KEYWORDS: Aegean; coastal evolution; micropalaeontology; palaeogeography; sea-level fluctuations.

Introduction

Around the end of the Holocene marine transgression, c. 6000 BP (Lambeck, 1996; Lambeck and Purcell, 2007), sea-level stabilization enabled ancient societies to settle along Mediterranean shores (Anthony et al., 2014; Murray-Wallace and Woodroffe, 2014; Vacchi et al., 2014, Vacchi et al., 2016a; Khan et al., 2015; Benjamin et al., 2017; Seeliger et al., 2017). For many civilizations, a connection to the sea was an important factor in establishing a flourishing settlement. In the Aegean, this statement is, for example, supported by the Neolithic settlements of Hoca Çeşme in Thrace (Başaran, 2010; Özbek, 2010), Hamaylıtarla on the Gallipoli peninsula (Özbek, 2010) and Çukuriçi Höyük near ancient Ephesus (Horejs, 2012; Horejs et al., 2015; Stock et al., 2015). All of them were situated <4 km from the sea, much closer than they are today (Ammerman et al., 2008). There are many examples from the Aegean that demonstrate that the fate of ancient settlements was closely linked to migrating shorelines and changing sea level. In western Anatolia, Troy, Miletos, Ainos, Ephesus and Liman Tepe are the most prominent examples. Their rise and fall as harbour cities were shaped by environmental changes, which have been described by many geoarchaeological studies (Kraft et al., 1977, 2007; Kayan, 1999, 2014; Brückner et al., 2006, 2013, 2015; Goodman et al., 2008, 2009; Delile et al., 2015; Shumilovskikh et al., 2016; Seeliger et al., 2018).

Here, we investigate the evolution of the coastal configuration around the city of Elaia that hosted the former military and commercial harbour of ancient Pergamon in Hellenistic and Roman times. Since 2013, several papers have focused on the environmental evolution of the Bay of Elaia. By analysing sediment cores taken inside and outside the main harbour basin of Elaia, the closed harbour, Seeliger et al. (2013) demonstrated how it was built in the first half of the 3rd century BC, how it has been used during the apogee of Elaia, and why it was abandoned due to massive sedimentation in late Roman times (see Fig. 2). Seeliger et al. (2014) used optically stimulated luminescence (OSL) dating and electrical resistivity tomography (ERT) measurements to probe the construction style and age of presently submerged walls c. 1–2 km south of the city and interpret these structures as the remains of saltworks constructed using spolia in Late Antiquity, a time when the harbours of Elaia were no longer navigable and the people had abandoned the city (Fig. 2a). Pint et al. (2015) performed detailed analyses of foraminifera and ostracoda, in combination with 3D-ERT measurements, to detect the style and usability of presumed Hellenistic ship sheds in the open harbour area of Elaia. They concluded that the open harbour and its ship sheds were operational during Hellenistic times, but were no longer navigable from Roman Imperial times onwards. Furthermore, Shumilovskikh et al. (2016) undertook a palynological investigation of sediment core Ela 70, taken from inside the closed harbour basin. They precisely reconstructed the palaeoenvironmental conditions and the vegetation history of the Bay of Elaia during the last

*Correspondence: E-mail: Martin Seeliger, as above.
E-mail: seeliger@em.uni-frankfurt.de

7500 a. Finally, Seeliger *et al.* (2017) described a new sea-level indicator based on foraminifera associations in the context of the transgressive contact. Based on these data, they reconstruct a relative sea-level (RSL) history for the area showing steadily rising sea-level since 7500 BP and today's sea-level maximum. By comparing their RSL history to curves from nearby Greek sites in the Aegean they reviewed the RSL evolution of the Aegean since the mid-Holocene. Furthermore, Feuser *et al.* (2018) recently published a summary presenting the state-of-the-art knowledge on the use of the Elaia's harbours, from an archaeological perspective.

In this article, we aim to integrate key findings of previous studies with new chronostratigraphic results to (i) investigate the causes of environmental modifications; (ii) reconstruct the changes in the shoreline of the Bay of Elaia; and (iii) provide fresh insights into the link between shoreline changes and human–environment interactions during Elaia's settlement period. Therefore, we focus on the period from 1500 BC onwards, which covers Elaia's prime as Pergamon's prospering harbour. In addition, we compare our results with other ancient coastal settlements in Asia Minor to provide a broader view on different environmental changes, which shaped the rise and fall of ancient coastal settlements in the eastern Aegean.

Physical setting

Elaia is located in the north-western part of modern Turkey (Fig. 1a,b). The study area is part of the westward-drifting Aegean–Anatolian microplate (Vacchi *et al.*, 2014). As a consequence of this drift, several E–W rift structures were formed in the late Miocene, such as the Bergama graben, and its tributary, the Zeytindağ graben. This tectonic ensemble represents a fractured zone, which was favourable to the evolution of the Kaikos valley (Vita-Finzi, 1969; Aksu *et al.*, 1987; Seeliger *et al.*, 2013; Fig. 1a). The Karadağ Mountains to the west and the Yuntdağ Mountains to the east border the Gulf of Elaia (Figs 1 and 2). The wide alluvial plain and the cuspate delta of the Bakır Çay (ancient name: Kaikos) are located to the west of the Bay of Elaia, separated by the flat ridge of Bozyertepe [40 m a.s.l. (above present sea level; Fig. 2)].

The Elaia coastal zone has a typical Mediterranean climate, Csa according to Koeppen and Geiger's nomenclature, with hot and dry summers, and mild and humid winters (Yoo and Rohli, 2016). Therefore, heavy rain and torrential rivers are major morphological agents (Brückner, 1994; Jeckelmann, 1996). Our own observations confirmed that the sea in the Bay of Elaia turns brownish due to excessive wash-down of colluvial material during heavy rains. Due to the steepness of the Yuntdağ Mountains, this effect is even stronger in the eastern part of the Bay of Elaia (Fig. 2c).

Historical background

Pergamon is one of the most famous ancient settlements in Turkey, frequently mentioned with Troy, Miletos, Ainos and Ephesus (Kraft *et al.*, 1980, 2003, 2007; Kayan, 1999; Brückner *et al.*, 2013; Seeliger *et al.*, 2018). Owing to shifts in the settlement areas, its impressive monumental structures, its important library and school of philosophers, Pergamon provides detailed insights into the urban structure of a Hellenistic city (Radt, 2016). Soon after Alexander the Great died in Babylon in 323 BC, the so-called 'Wars of the Diadochi' affected great tracts of his empire (Cartledge, 2004). In a later stage of these fights, the dynasty of the *Attalids* came to power in the Kaikos region and established — in alliance with Rome — a powerful kingdom in Asia Minor, which, during its prime under King Eumenes II (197–159 BC) ruled the western half of present-day Turkey. In 133 BC, their realm was integrated into the growing Roman Empire (Hansen, 1971; Pirson and Scholl, 2015; Radt, 2016; Fig. 1c). Pergamon's location on top of the 330-m-high Acropolis hill, overlooking the surrounding Kaikos plain, was excellent for security and defence, but complicated trade and transport. Furthermore, the Pergamenians were in need of a maritime harbour. They found it in the nearby city of Elaia, located on the Aegean Sea approximately 26 km south-west of Pergamon (Figs 1a and 2a). According to current research knowledge, Elaia came under Pergamenian hegemony during the regency of Eumenes I (263–241 BC; Pirson, 2004; Radt, 2016). Additionally, *Strabo* mentioned Elaia as the commercial harbour of the Pergamenians and as the military base of the *Attalids* (*Geographica XIII, 1, 67; XIII, 3, 5*). Further evidence from literary sources and archaeological findings emphasizes the close link between Elaia and Pergamon (Pirson, 2004, 2008, 2010, 2011, 2014). The harbour zone of Elaia was divided into three parts (Fig. 2).

First, the closed harbour basin (I in Fig. 2) within the fortification walls, was built in early Hellenistic times. It was protected from the sea and enemy attacks by two massive breakwaters; today they are landlocked, but still visible. Geoarchaeological research has revealed that substantial siltation occurred between the 3rd and the end of the 4th centuries AD; from the 5th century AD onwards the closed harbour was no longer navigable (Pirson, 2007, 2008; Seeliger *et al.*, 2013, 2017). Second, a c 250-m-long open harbour zone (II in Fig. 2) stretched from the southern breakwater of the closed harbour south-eastwards to the point where an internal wall reached the waterfront. This so-called *diateichisma* divided the city area into a northern, densely populated part and a southern one (Pirson, 2011; Pint *et al.*, 2015). Third, a beach harbour extended from south of the diateichisma to the south-eastern tip of the city wall (III in Fig. 2). This area was probably used as a multifunctional military zone, including dockyards where warships were beached and maintenance work was conducted (Pirson, 2011, 2014; Pint *et al.*, 2015).

Palaeogeographical research was conducted to assess small-scale palaeoenvironmental changes in the Bay of Elaia. Because Elaia served as the satellite harbour city of Pergamon during its prime, previous research focused on the function and temporal use of the different harbours identified (Seeliger *et al.*, 2013, 2017; Pint *et al.*, 2015). Although detailed research was conducted, some key questions remain. Key knowledge gaps include: (i) How did coastal and RSL changes influence the human occupation history of the city? (ii) To what extent does Elaia fit with the traditional 'rise and fall model' linked to shoreline migration?

Seeliger *et al.* (2017) took a first step towards answering these questions, by publishing an RSL curve for Elaia and comparing it to the RSL histories of other study areas in the Aegean. Here we seek to further explore the role of Elaia as an example of shoreline migration and human settlement changes in the Aegean during ancient times. This research is based on 19 sediment cores, drilled along five transects perpendicular to the present shoreline (Fig. 2a). This approach has been widely adopted in Mediterranean coastal studies (e.g. Kraft *et al.*, 2007; Goodman *et al.*, 2008, 2009; Kayan, 2014; Marriner *et al.*, 2014; Delile *et al.*, 2015; Morhange *et al.*, 2016; Evelpidou *et al.*, 2017; Flaux *et al.*, 2017; Giaime *et al.*, 2017; Pennington *et al.*, 2017; Seeliger *et al.*, 2018) to investigate lateral and vertical changes in the
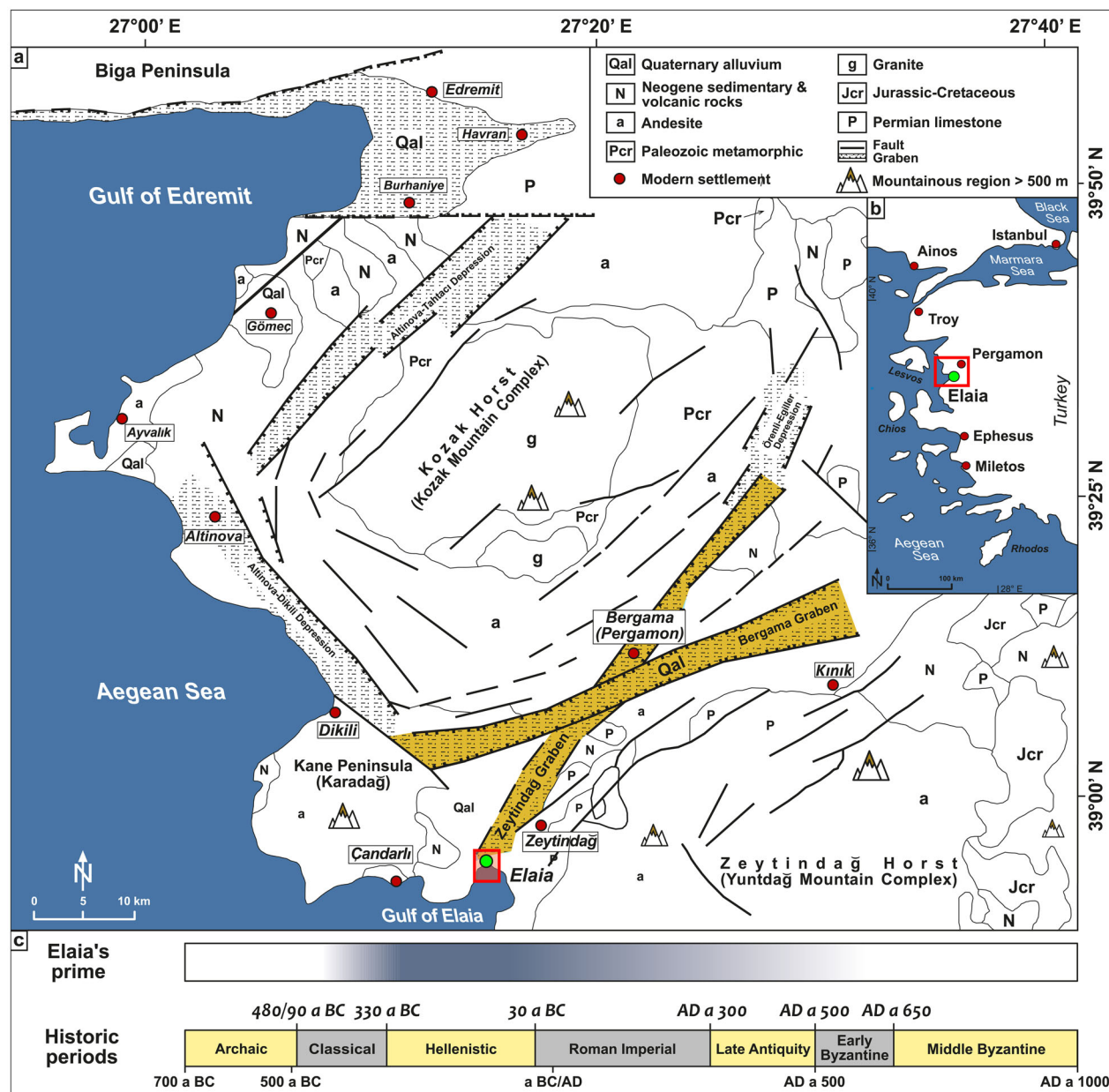
Figure 1. The study area on the Aegean coast of Turkey. (a) Structural map and surrounding mountain ranges. Bergama and Zeytindağ grabens are marked in yellow. The study area of Elaia (Fig. 2a) is denoted in pale red. Source: Altunkaynak and Yılmaz (1998), substantially modified, with locations mentioned in the text. (b) General map of the Turkish Aegean coast with the position of the study area (Fig. 1a) and further ancient settlements mentioned in this paper. Source: Radt (2016), substantially modified. (c) Timeline of the historical periods, linked to the period of Elaia's prime (based on Pirson and Scholl, 2015; Radt, 2016).

sediment stratigraphy and to probe the evolution of the landscape, notably shoreline migration.
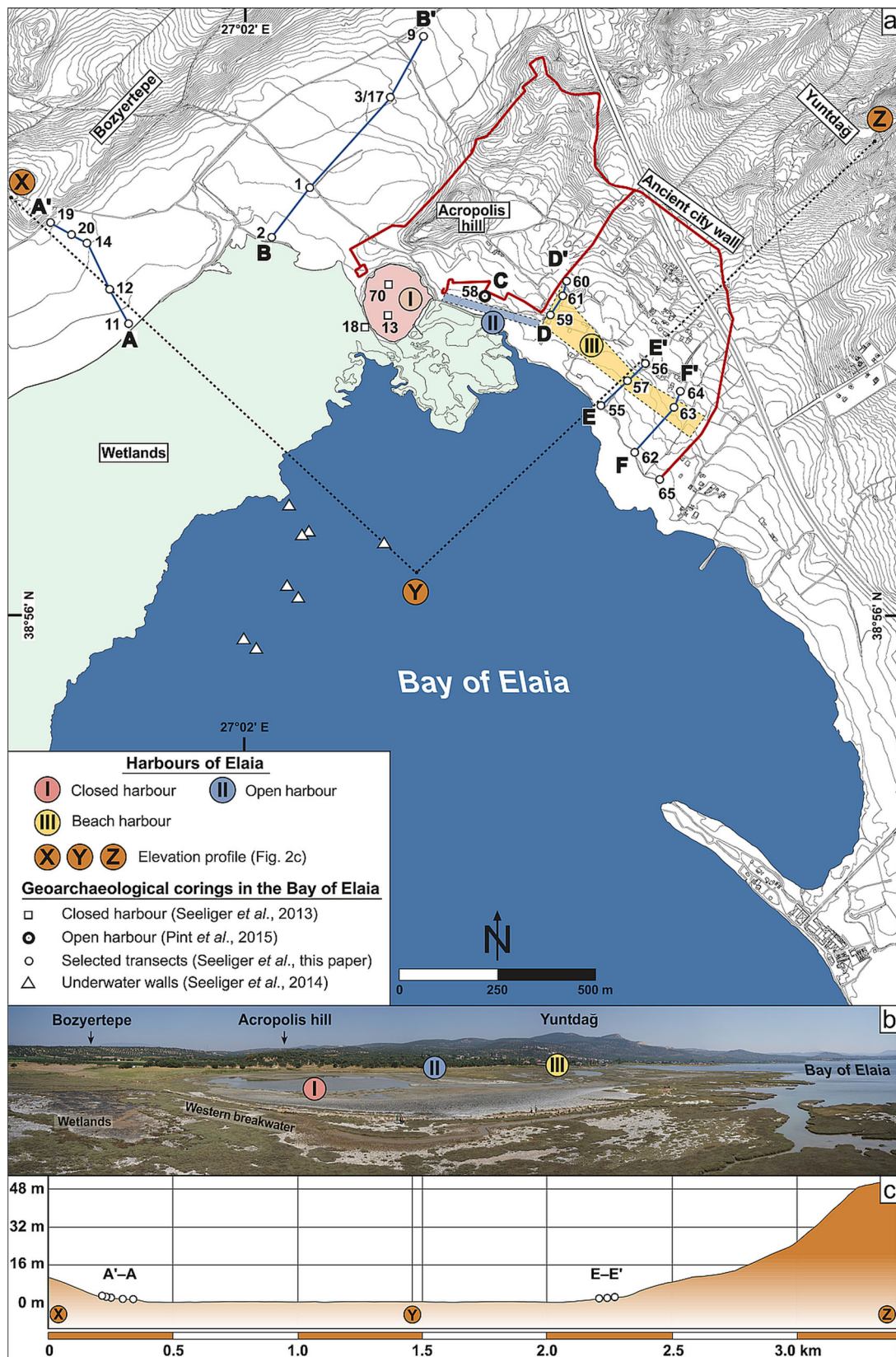
Material and methods

Geoarchaeological fieldwork

Sediment cores were extracted using an Atlas Copco Cobra TT vibracorer with open steel auger heads (diameter of 6 and 5 cm, respectively) in the surroundings of the Bay of Elaia, down to a maximum depth of 12 m b.s. (below the surface). On-site, sediments were described according to grain size and colour (Ad-hoc-AG Boden, 2005; Munsell Soil Color Charts) and bulk samples for laboratory analyses were taken from the open sediment cores (5–6 samples m^{-1}). All coring sites were georeferenced using a Leica DGPS System 530 (accuracy of ≤2 cm in all three dimensions; Seeliger et al.,

2013, 2014); they are reported in metres above sea level (a.s. l.) and metres below the surface (b.s.).

Sedimentology and geochemistry

Multi-proxy laboratory analyses were conducted (Ernst, 1970; Hadler et al., 2013; Seeliger et al., 2013, 2018; Bartz et al., 2015, 2017). Samples were air-dried and sieved to separate the ≤2-mm grain-size fraction for further analyses. For laser-based grain-size analysis (Beckman Coulter LS13320), the organic content was decomposed using 15% hydrogen peroxide (H_2O_2). Afterwards, sodium pyrophosphate ($Na_4P_2O_7$; concentration: 47 g L^{-1}) was taken as a dispersant. Each sample was measured three times in 116 classes, determining grain-size distributions in a range from 0.04 to 2000 μm. For the calculation of grain-size parameters (Folk and Ward, 1957), we used the software package GRADISTAT

Figure 2. Locations of selected vibracores taken in the Bay of Elaia. (a) Locations of coring transects A–A', B–B', D–D', E–E' and F–F', 'C' (coring Ela 58), and of the elevation profile XYZ shown in (c). (b) Panoramic view of the study area (UAV image; taken on 1 September 2015 by A. Bolten) with the location of the harbour areas. (c) Elevation profile XYZ (based on Google Earth Pro; 21 July 2018). The enhanced relief energy of the eastern part in contrast to the western area of the Bay of Elaia is clearly evident.

(Blott and Pye, 2001). To estimate the organic content, measurements of loss on ignition (LOI) were performed by oven drying (105 °C for 12 h to determine the water content) and combustion in a furnace (550 °C for 4 h to determine the

organic substance). Electric conductivity was measured in an aqueous solution (5 g of sediment in 25 mL deionized water) with a glass electrode connected to a Mettler Toledo InLab 731-2m instrument. To determine different sedimentary units,

Table 1. Radiocarbon data sheet. ^{14}C-AMS dating was carried out at the Centre for Applied Isotope Studies (CAIS) of the University of Georgia in Athens, USA (lab. code: UGAMS) and the [14]Chrono Centre for Climate, the Environment, and Chronology, Queen's University Belfast, UK (lab. code: UBA). All ages were calibrated with the IntCal13 or Marine13 calibration curves depending on sample δ^{13}C using the recent Calib 7.1 software (Reimer *et al.*, 2013). A marine reservoir effect of 390 ± 85 years and a ΔR of 35 ± 70 years (Siani *et al.*, 2000) was applied. The calibrated ages are presented in calendar years BC/AD and years BP with 2σ confidence interval.

Sample name	Lab. code	Sample type	Depth b.s.	Depth b.s. l.	δ^{13}C (‰)	[14]C age (a $\pm 1\sigma$)	cal a BC/cal a AD (2σ)	cal a BP (2σ)
Ela 2/9	UGAMS 4148	Shell (*Nucula* sp.)	2.94 m	2.71 m	4.20	2236 ± 27	30 BC to AD 347	1603–1979 BP
Ela 2/22SG	UGAMS 4150	Seagrass	9.56 m	9.33 m	−12.72	3194 ± 28	1201–816 BC	2765–3150 BP
Ela 3/7H	UGAMS 4151	Wood	4.28 m	0.47 m	−24.4	305 ± 52	AD 1458–1793	157–492 BP
Ela 3/12H	UGAMS 4152	Seagrass	4.98 m	1.17 m	−13.6	4176 ± 30	2460–2032 BC	3981–4409 BP
Ela 3/15	UGAMS 4153	Shell (*Lasaea rubra*)	5.80 m	1.99 m	2.4	6606 ± 31	5304–4946 BC	6895–7253 BP
Ela 12/36H	UGAMS 6039	Charcoal	8.65 m	7.77 m	−26.7	2560 ± 25	803–568 BC	2517–2752 BP
Ela 14/10H	UGAMS 6035	Wood	3.75 m	2.49 m	−25.8	2440 ± 25	750–409 BC	2358–2699 BP
Ela 14/18	UGAMS 6034	Seagrass	6.36 m	5.10 m	−14.3	5300 ± 25	3877–3516 BC	5465–5826 BP
Ela 17/14H	UGAMS 6033	Charcoal	4.90 m	1.57 m	−24	3640 ± 25	2129–1929 BC	3878–4078 BP
Ela 18/7HK	UGAMS 6031	Charcoal	1.38 m	1.20 m	−24.5	1740 ± 25	AD 240–380	1570–1710 BP
Ela 20/15	UGAMS 6028	Seagrass	3.85 m	2.47 m	−15.9	3180 ± 25	1183–807 BC	2756–3132 BP
Ela 20/16SG	UGAMS 6027	Piece of bark	4.04 m	2.66 m	−14.5	3350 ± 25	1735–1536 BC	3485–3684 BP
Ela 57/8H	UGAMS 11 900	Olive seed	1.95 m	0.86 m	−26.6	1960 ± 25	38 BC to AD 116	1834–1987 BP
Ela 57/17H	UGAMS 11 901	Grape seed	3.56 m	2.47 m	−25.3	2060 ± 25	165 BC to 1 BC/AD	1949–2114 BP
Ela 57/23H	UGAMS 11 441	Charcoal	5.39 m	4.30 m	−27.4	3720 ± 25	2198–2035 BC	3984–4101 BP
Ela 58/14HK	UGAMS 11 442	Charcoal	2.73 m	1.84 m	−26.7	2080 ± 25	175–41 BC	2124–1990 BP
Ela 58/17H	UGAMS 11 443	Melon seed	3.30 m	2.41 m	−25.0	2020 ± 25	91 BC to AD 52	2040–1898 BP
Ela 58/24Po	UGAMS 11 444	Seagrass	4.40 m	3.51 m	−10.8	2740 ± 25	731–299 BC	2680–2248 BP
Ela 58/32	UGAMS 11 445	Seagrass	7.75 m	6.86 m	−16.2	6170 ± 30	4796–4439 BC	6745–6388 BP
Ela 58/38F	UGAMS 11 446	Charcoal	8.35 m	7.46 m	−26.1	6920 ± 30	5876–5731 BC	7825–7680 BP
Ela 61/16	UBA 28 500	Bulk of marine ostracoda	5.60 m	2.34 m	0.1	3154 ± 23	1149–791 BC	2740–3098 BP
Ela 61/19	UGAMS 11 448	Charcoal	6.70 m	3.34 m	−27.4	3570 ± 25	2016–1784 BC	3733–3965 BP
Ela 63/10H	UGAMS 11 903	Charcoal	4.54 m	2.23 m	−28.0	2540 ± 25	797–551 BC	2500–2746 BP
Ela 63/485	UBA 28 499	Bulk of marine ostracoda	4.85 m	2.54 m	8.0	2952 ± 27	903–501 BC	2450–2852 BP
Ela 63/11	UGAMS 11 904	Charcoal	4.88 m	2.57 m	−28.0	2640 ± 25	834–792 BC	2741–2783 BP

characteristic elements (Fe, K, Ca, Ti, etc.) were measured using a portable X-ray fluorescence (XRF) spectrometer (Niton Xl3t 900 GOLDD; Vött *et al.*, 2011; Lubos *et al.*, 2016). To ensure comparability with all XRF analyses and to reduce grain-size dependency, each sample was ground to powder in a ball triturator (Retsch PM 4001) and then pressed into pills.

Micropalaeontology

For microfaunal analysis, selected 1-cm^3 samples were wet-sieved using a 100-µm mesh. Under a stereoscopic microscope, at least 300 ostracod valves and foraminifer tests, respectively, were picked from appropriate splits of the residues of every sample. If fewer than 300 specimens were present within a sample all were picked. Species were identified and counted according to Bonaduce *et al.* (1975) and Joachim and Langer (2008) for ostracods as well as Cimerman and Langer (1991), Meriç *et al.* (2004) and Murray (2006) for foraminifers.

Chronology

The chronological framework is based on ^{14}C accelerator mass spectrometry (AMS) age determinations. Depending on the δ^{13}C value, each sample was calibrated using either the IntCal13 or the Marine13 calibration curve in Calib 7.1 (Reimer *et al.*, 2013) with a marine reservoir age of 390 ± 85 a and a ΔR of 35 ± 70 a (Siani *et al.*, 2000). Siani *et al.* (2000) used shells of known age sampled in the Dardanelle Strait and stored in the Muséum National

d'Histoire Naturelle, Paris, to calculate the local marine reservoir age and its ΔR. As there are no further studies in the closer vicinity of Elaia, this value has been chosen to correct the calibrations on marine material. Finally, because the spatiotemporal variation of the marine reservoir effect for the Aegean is still not completely understood, the ^{14}C ages of marine carbonates should be interpreted carefully. Because this paper presents archaeological-related data, all ages are presented in cal a BC/AD. Table 1 provides all mentioned ages in cal a BP.

Results of Ela 57 and Ela 12

The coring profiles of the Elaia region, of which a selection of 19 is presented here (Fig. 2a), can be divided into two groups: those, which reach bedrock and those that do not. Additionally, the sedimentation pattern in the western part of the Bay (transects A–A′ and B–B′) differs significantly from that of the eastern part (D–D′, E–E′ and F–F′). This is demonstrated by the detailed description of two cores, one from each group: Ela 57 (Figs 3 and 4) and Ela 12 (Figs 5 and 6). Additionally, Ela 58 (Pint *et al.*, 2015) is considered to present all sedimentary units (Fig. 2a). A detailed description of the profiles Ela 57 and Ela 12 is given in Supporting Information *Appendix* S1.

Interpretation

Introduction of sedimentary units

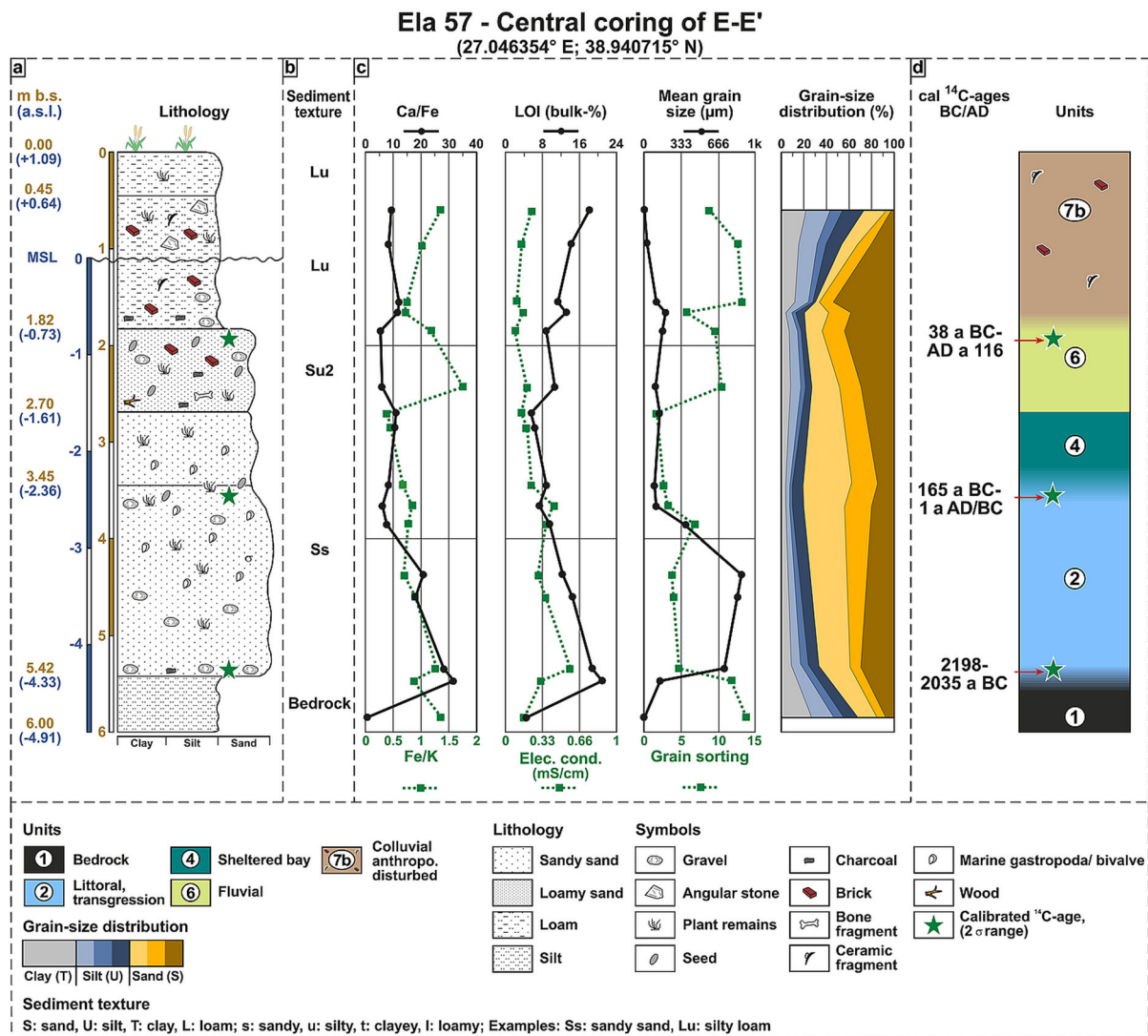Many sediment cores from the Elaia area are summarized based on classification in units of typical environmental

Figure 3. Sediment core Ela 57 with geochemical and sedimentological parameters (a, b, c). (d) Interpretation of sedimentary units and dating results.

characteristics. Their definition is based on geochemical, granulometric and micro-faunistic parameters of cores Ela 57 and 12. This compilation is intended to shorten the interpretation of the cores (Fig. 7) and described in detail in *Appendix S2*.

Sediment core-based reconstruction of palaeoenvironments

Based on the previous sections, coring profiles Ela 57 and Ela 12 are interpreted as follows.

Sediment core Ela 57 representing the eastern part of the Bay of Elaia

The palaeogeographical evolution of the eastern part of the Bay of Elaia is exemplified by Ela 57 (Figs 2–4).

Neogene bedrock (unit 1), encountered at 5.42 m b.s., forms the base of numerous cores in the study area. The calcareous sandstone, outcropping nearby, was used to construct the harbour breakwaters (Seeliger *et al.*, 2013, 2014). The overlying unit 2 represents the transgressive littoral unit during the Holocene sea-level rise. The high-energy environment is clear from a number of gravels, the coarse grain size and patches of seagrass. The low

biodiversity and the sole occurrence of robust foraminifers in the lower part of unit 2, such as *Ammonia compacta* and *Elphidium crispum*, are evidence for the high stress level of this littoral environment in which only a few species are able to survive (Seeliger *et al.*, 2017). The fining-upward sequence is due to increasing water depth, which is also reflected by a higher biodiversity. The Holocene transgression reached this area at the end of the third millennium BC (2198–2035 cal a BC), which is far before the human occupation phase of Elaia. The second age of Ela 57 dates to late Hellenistic/early Roman times (165 cal a BC to 1 cal a BC/AD), the period when Elaia flourished. Rising sea level led to the formation of a shallow water body represented by unit 4. This shows a fining-upward sequence due to inland migration of the shoreline, leading to reduced wave action. This results in a lower amount of shell debris and the occurrence of preserved valves. The microfaunal association indicates a shallow marine environment. Based on our results from within the closed and open harbours, relative sea level around the birth of Christ was approximately 1.50 m lower than today. Thus, water depth at this time should not have exceeded more than 1.30–1.50 m (Pint *et al.*, 2015; Seeliger *et al.*, 2017).

By then, the surroundings of this part of the city may have served as a beach harbour where foreign soldiers landed and
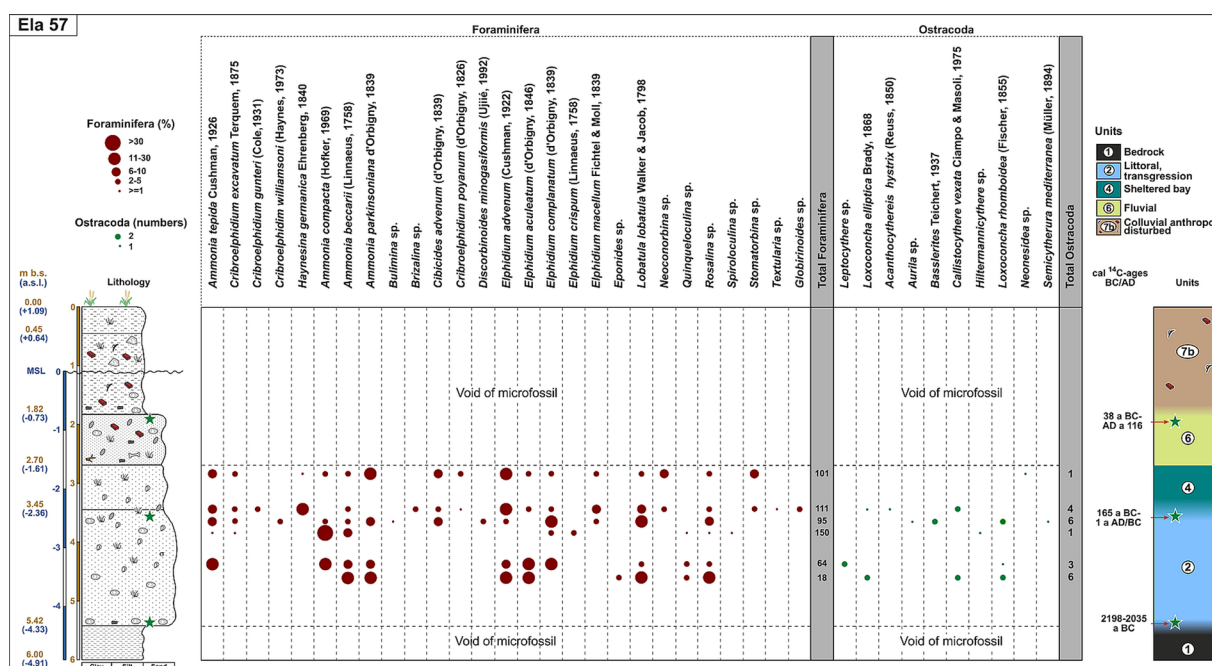
Figure 4. Sedimentary units of core Ela 57, based on microfauna. Relative abundance of ostracods and foraminifers is given semiquantitatively.

repaired their ships and put up camp, thus remaining outside the area of the actual city. This custom was normal for small to medium-sized cities at this time, because it offered a higher level of security for the inhabitants. As the nearby core Ela 56 does not show any marine or littoral sediments, the site of Ela 57 always lay in a nearshore position, close to the landing area for ships and smaller vessels. A sharp contact at −1.61 m a.s.l. suggests a sudden end to this sheltered marine water body, possibly due to massive deposition engendered by torrential floods, triggered by heavy rainfall. Such erosional events may have been favoured by widespread deforestation of this area during Hellenistic and Roman times (Shumilovskikh *et al.*, 2016). The erosional contact at the base, fining-upward sequence, fluvial character of the stratum including brick fragments, seeds, charcoal and even bones, all washed down from the nearby slopes, as well as absence of microfauna support this interpretation. The upper part of this unit dates to Roman Imperial times. Since the dated olive stone (Ela 57/8H; Table 1) is very robust and may have been reworked, the age should should be regarded as a minimum one. Fluvial deposition probably occurred during the final phase of the settlement of Elaia in late Roman times and may have influenced the final decision to abandon the city. Since the area around coring site Ela 57 suddenly became terrestrial, the second transition of the shoreline, often indicated by a second littoral phase (unit 5), is missing. That the area was at least partly influenced by human impact is evidenced by the anthropogenically disturbed colluvium (unit 7b), which forms the top layer.

Sediment core Ela 12 representing the western part of the Bay of Elaia

The palaeogeographical evolution of the western Bay of Elaia is exemplified by profile Ela 12 (Figs 2, 5 and 6).

At the base, the profile shows sediments of a sheltered embayment (unit 4) where *Posidonia oceanica* meadows could thrive on the sea floor (Vacchi *et al.*, 2016b). Well-preserved marine bivalves support this idea. The geochemical data and microfaunal association indicate a near-shore environment as typically open-marine species are missing (Pint *et al.*, 2015). A radiocarbon age of 803–568 cal a BC dates this part to the first half of the first millennium (Geometric-Archaic times). Very little is known about the history of the study area during this period (Pirson and Scholl, 2015; Fig. 1c). The shallow marine environment prevailed for some time until sediments from the nearby Bozyertepe were increasingly washed into the embayment. This caused a regression of the shoreline with decreasing water depth, and the establishment of littoral unit 5, which is of progradational origin. Compared to the transgressive unit 2 of Ela 57, the progradational unit 5 of Ela 12 has a similar microfaunal composition but displays a coarsening-upward sequence. Environmental stress led to low biodiversity, while the increased occurrence of mollusc and shell debris provides evidence of intense wave energy. The advancing delta of the Kaikos (Bakır Çay) do not play a major role in the silting up of this inner part of the Bay of Elaia given that neither Ela 12 nor the whole transects A–A′ and B–B′ contain fluvial–deltaic sediments and the Bozyertepe acts as a barrier for this material (Fig. 2a). The littoral unit ends at −2.78 m a.s.l., when terrestrial processes become dominant. This marks the onset of the accumulation of colluvium (unit 7a). Since transect A–A′ is situated at a distance from the settled area of Elaia, it is not surprising that no direct indicators of human impact are found inside the colluvium.

Landscape evolution based on coring transects

Following the detailed description description of two representative sediment cores, five transects and one single coring are discussed to clarify the landscape evolution of the Bay of Elaia (Fig. 8).

Transect A–A′ consists of three different types of profiles. The coastal corings Ela 11 and 12 show a typical regressive sedimentary sequence (Fig. 8). Increased sedimentation in the context of the settlement period of Elaia led to the silting up of a low-energy, shallow-marine water body (unit 4), developing into a littoral progradation unit 5 and later to a natural colluvial environment (unit 7a). Ela 14 and 20 reach bedrock,
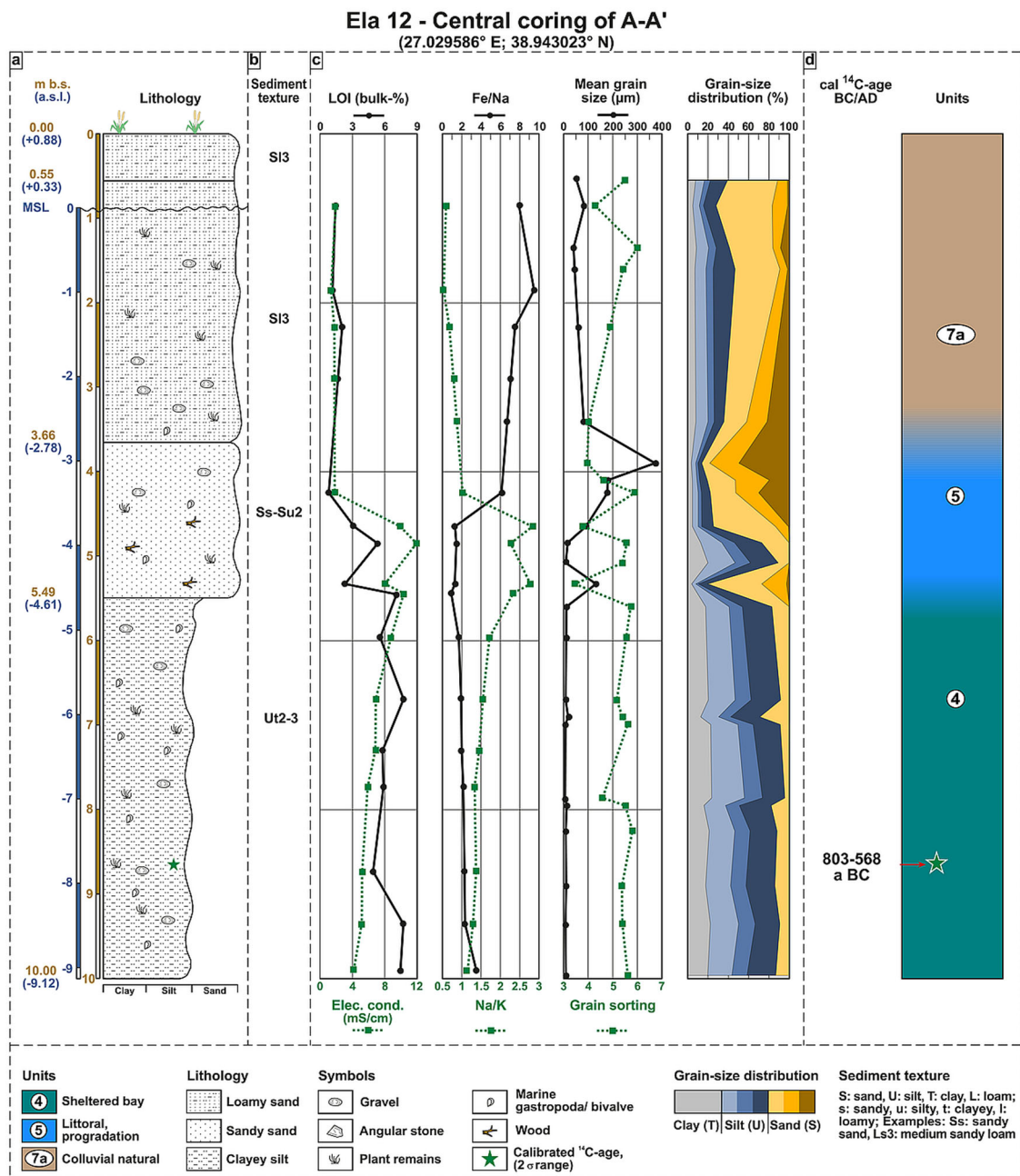
Figure 5. Sediment core Ela 12 with geochemical and sedimentological parameters (a, b, c). (d) Interpretation of sedimentary units and dating result.

which is topped by nearshore littoral deposits (unit 2); these are overlain by natural colluvium. The rising bedrock towards the Bozyertepe causes the landward thinning of the littoral strata. Since core Ela 19 does not contain marine, fluvial or littoral units, the maximum marine transgression in A–A' is close to coring Ela 20, where it is dated to the end of the second millennium BC. Transect B–B' represents the marine transgression into the valley between the Acropolis to the east and the Bozyertepe to the west (Fig. 8). It provides results comparable to transect A–A'. Coastal corings Ela 1 and 2 demonstrate a regressive sedimentary sequence, similar to Ela 11 and 12. They represent a shallow water body in this area of the Bay of Elaia at least since the first half of the first millennium BC. According to these results, the areas of Ela 1 and 2 were still under marine influence during the main occupation phase of Elaia (Figs 1c and 2). Since Ela 9 only contains colluvial sediments, coring Ela 3/17 marks the

maximum marine transgression of B–B'. This dates to the end of the third millennium BC. Ela 58 ('C') is the only core in this area, which includes a shallow marine unit (unit 3) with high biodiversity. It dates to the fourth/fifth millennia BC. As in the eastern transects, massive fluvial input ended the shallow marine conditions and initiated a sheltered water area (unit 4), which prevailed throughout Elaia's main phase. Later, the Elaitians dumped material in this area to consolidate the terrain. Transects D–D', E–E' and F–F' show similar results, and are therefore presented together. The nearshore coring profiles (Ela 59, 55 and 62) reach bedrock. The transgressive littoral unit 2, starting with an erosional disconformity, is covered by unit 4 of a stagnant marine water body. Very low-energy wave conditions prevailed because a progradational unit 5 is missing; all the profiles show a smooth transition to colluvial deposits (unit 7a). The inland corings (Ela 60, 56 and 64) reveal a terrestrial sedimentation pattern interrupted by a layer
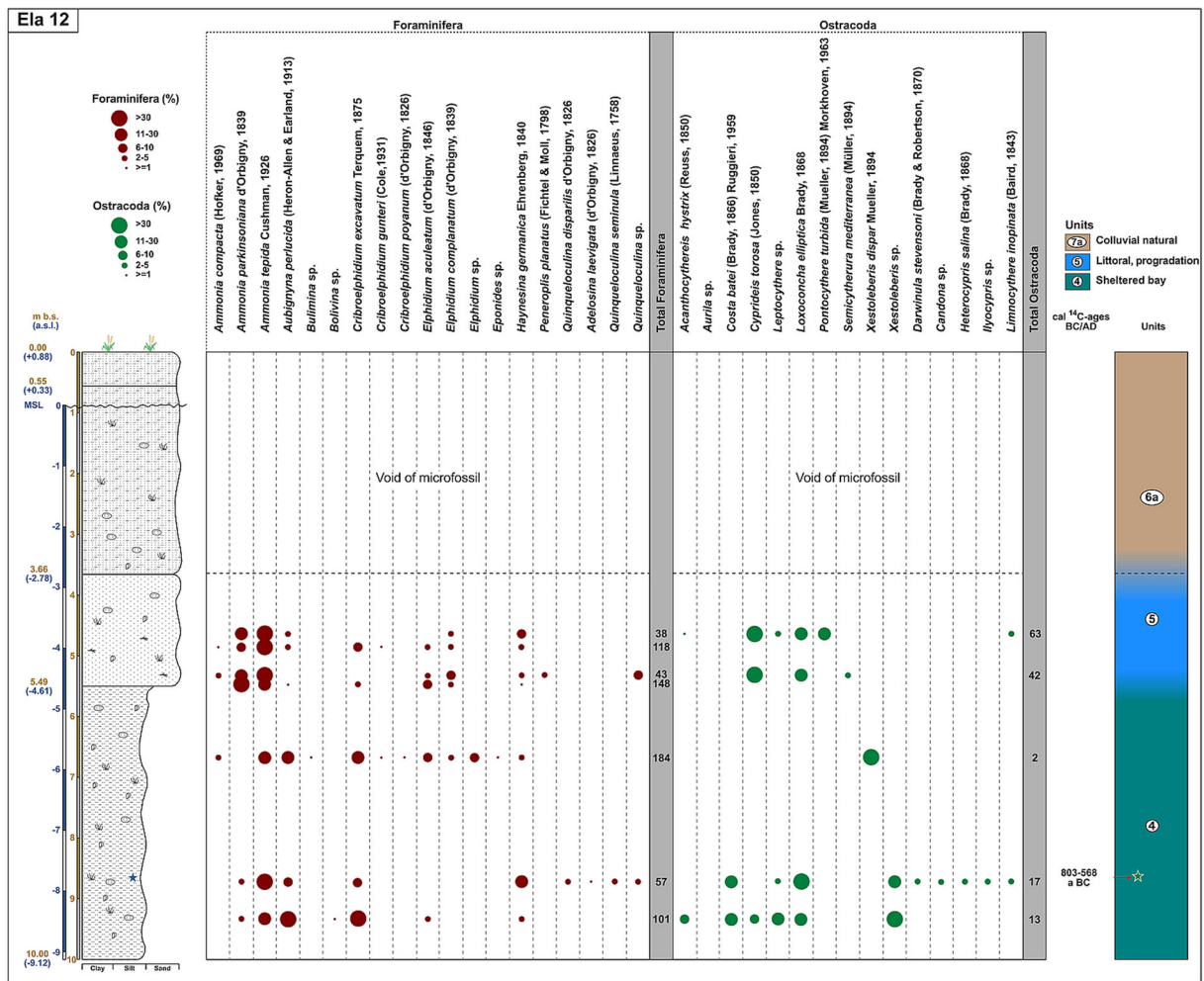
Figure 6. Sedimentary units of core Ela 12, based on microfauna. Relative abundance of ostracods and foraminifers is given semiquantitatively.

of fluvial sediments, probably caused by torrential floods. The central corings (Ela 61, 57 and 63) contain key information regarding the marine extension in this area. All display a typical stratigraphy: the bedrock is overlain by transgressive littoral deposits; then units of a low-energy marine embayment follow and provide evidence of the rising sea level. The shallow-marine deposit is covered by massive input of fluvial sediments, which are topped by human-induced colluvium. Severe flooding can only be traced in the sediment sequence of the central and inland corings (Seeliger *et al.*, 2017).

Synopsis

With regard to the height above sea level in F–F′, a similar age for the maximum marine ingression in each transect of *c.* 1500 BC is assumed. Derived from the thickness of the marine strata of Ela 58 ('C'), the maximum transgressive shoreline is probably located further inland, *i.e.* in the area of the later city (where coring was not possible). Ela 61 indirectly proves this assumption. This is comparable to other ancient cities such as Miletos, Ainos and Ephesus where parts of the cities were also erected on former marine sediments (Brückner *et al.*, 2006, 2015; Kraft *et al.*, 2007; Seeliger *et al.*, 2018). The eastern city district transects and Ela 58 ('C') show thick sheet-wash deposits which caused massive siltation of the area. In the case of Ela 58, this could have taken place at the beginning of the first millennium BC. This is in good agreement with transect D–D′ where this event occurred at a similar date (Ela 61/16; 1149–791 cal a BC). In Ela 57 (E–E′), it

is visible just around the birth of Christ, whereas in Ela 63 (F–F′) it occurred in Classical or even Hellenistic times (shortly after Ela 63/10/H; 797–551 cal a BC). However, severe flood events did not occur in the western part of the embayment (transects A–A′ and B–B′). In summary, torrential floods associated with sheet-wash dynamics occur before and during the period of intense human settlement activity; they affected the eastern area of ancient Elaia (Fig. 2). This is, on the one hand, a result of the topography of the nearby foothills of the steep Yuntdağ Mountains, as compared to the flat Bozyertepe and the Acropolis (A–A′ and B–B′; Fig. 2). On the other hand, the human influence in the eastern part of the embayment was more intense, leading to degradation of the vegetation cover, soil degradation and erosion. At the end of the first century BC and the beginning of the first century AD the pattern of settlement of the area around Elaia changed when several of the Hellenistic farmsteads were abandoned – perhaps because of intense floods (Pirson, 2011).

Scenarios of shoreline changes

Based on these results, we reconstructed the palaeogeography of the Bay of Elaia for three different time periods (1500 BC, 300 BC and AD 500; Figs 2 and 9).

1500 BC

This is the time of the maximum marine extension in the Bay of Elaia, when sea level was 3.3–2.4 m lower than today (Seeliger *et al.*, 2017). The coastal zone reached northwards
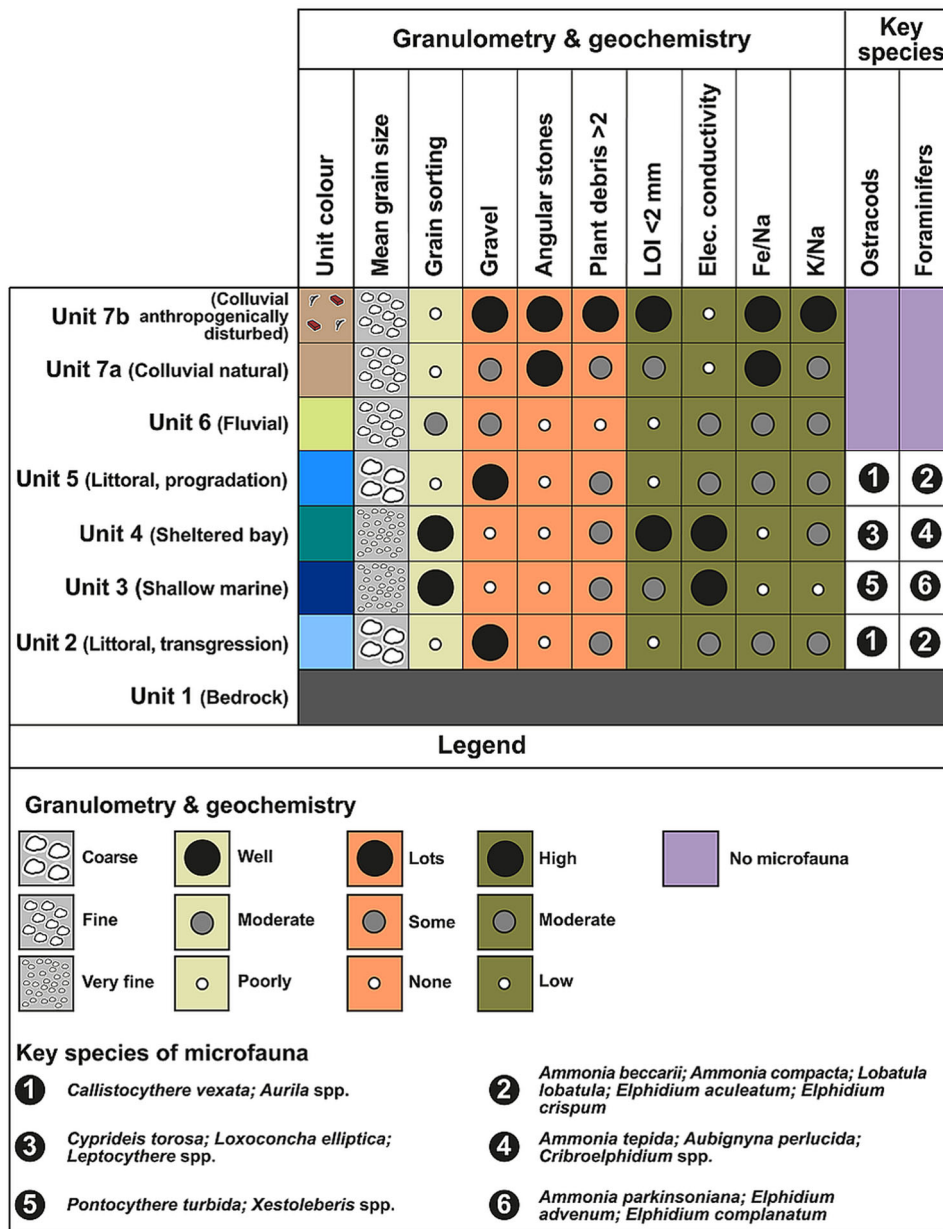
Figure 7. Microfaunal, granulometric and geochemical characteristics of the sedimentary units of the corings in the Bay of Elaia. Because these characteristics are dependent on regional factors (bedrock, weathering conditions, etc.) care should be exercised before transposing these data to other study areas.

along the slopes of Bozyertepe, almost up to Ela 9 where one of Elaia's cemeteries was located (Pirson, 2010). This supports the idea that the sea never transgressed this area during the Holocene. During the maximum marine extension, the later Acropolis of Elaia protruded into the bay as a peninsula. Nonetheless, it was most probably uninhabited at this time. The small embayment to the north of Ela 58 may have acted as a preferred landing area, but this assumption has not yet been verified by archaeological finds. The same holds true for the western flank of the Acropolis. In the eastern city area, the shoreline lay close to the foothills of the Yuntdağ. The former shallow-marine and littoral areas of the later city are easy to identify. Once these had silted up, and probably also partly filled in by the city's inhabitants, they evolved into settled ground after c. 500 BC (Figs 2 and 9).

300 BC

This scenario represents the period when Elaia started to prosper, when sea level was just 1.6–2.0 m lower than today (Seeliger et al., 2017). Archaeological findings document

intense human activities on the Acropolis and in the eastern city district (Pirson, 2010). In addition, palynological data show that various crops were intensively cultivated in the areas surrounding Elaia (Shumilovskikh et al., 2016).

Increased sediment load due to soil erosion from Bozyertepe and minor activities of a unnamed ephemeral creek between Bozyertepe and Acropolis caused shoreline regression in the western part. None of the corings of A–A' and B–B' show fluvial sediments of the nearby Kaikos delta. Therefore, its influence on siltation of the inner part of the Bay of Elaia can be neglected. Wide areas between the Acropolis and Bozyertepe remained marine. Due to the ongoing seaward shift of the shoreline, a harbour on the western flank of the Acropolis hill is unlikely at this time. Immediately south of the Acropolis, two harbours were constructed: the local geomorphology was consolidated and transformed into a closed harbour basin with the erection of two breakwaters (Seeliger et al., 2013). Water depth in the closed harbour basin was c. 2.5 m, sufficient for all common battle and merchant ship classes used by the Pergamenians at that time (Seeliger et al., 2017). Similar considerations also
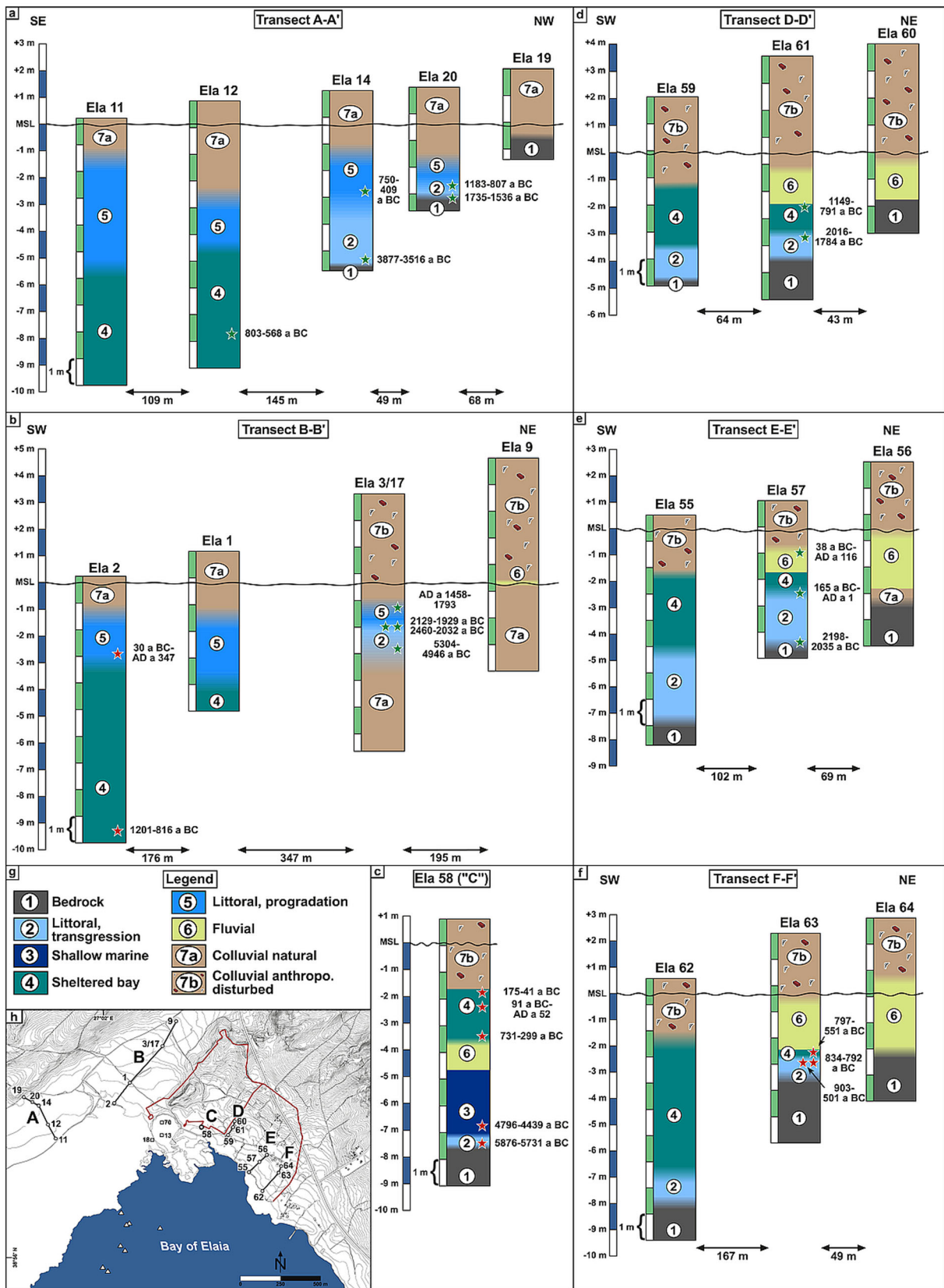
Figure 8. Synopsis of the coring transects (a) A–A', (b) B–B', (d) D–D', (e) E–E' and (f) F–F', as well as (c) (Ela 58); (g) legend; (h) locations of corings and transects.

hold true for the area of the open harbour, including the presumed Hellenistic ship sheds where water depth was c. 1.2 m (Pirson, 2010; Pint et al., 2015; Seeliger et al., 2017). As this area was essentially used to haul vessels into the ship sheds, water depth must have been sufficient to operate ship

sheds. In summary, both harbours were fully accessible and used for military and commercial purposes at this time (Pirson, 2004; Pint et al., 2015; Seeliger et al., 2017).

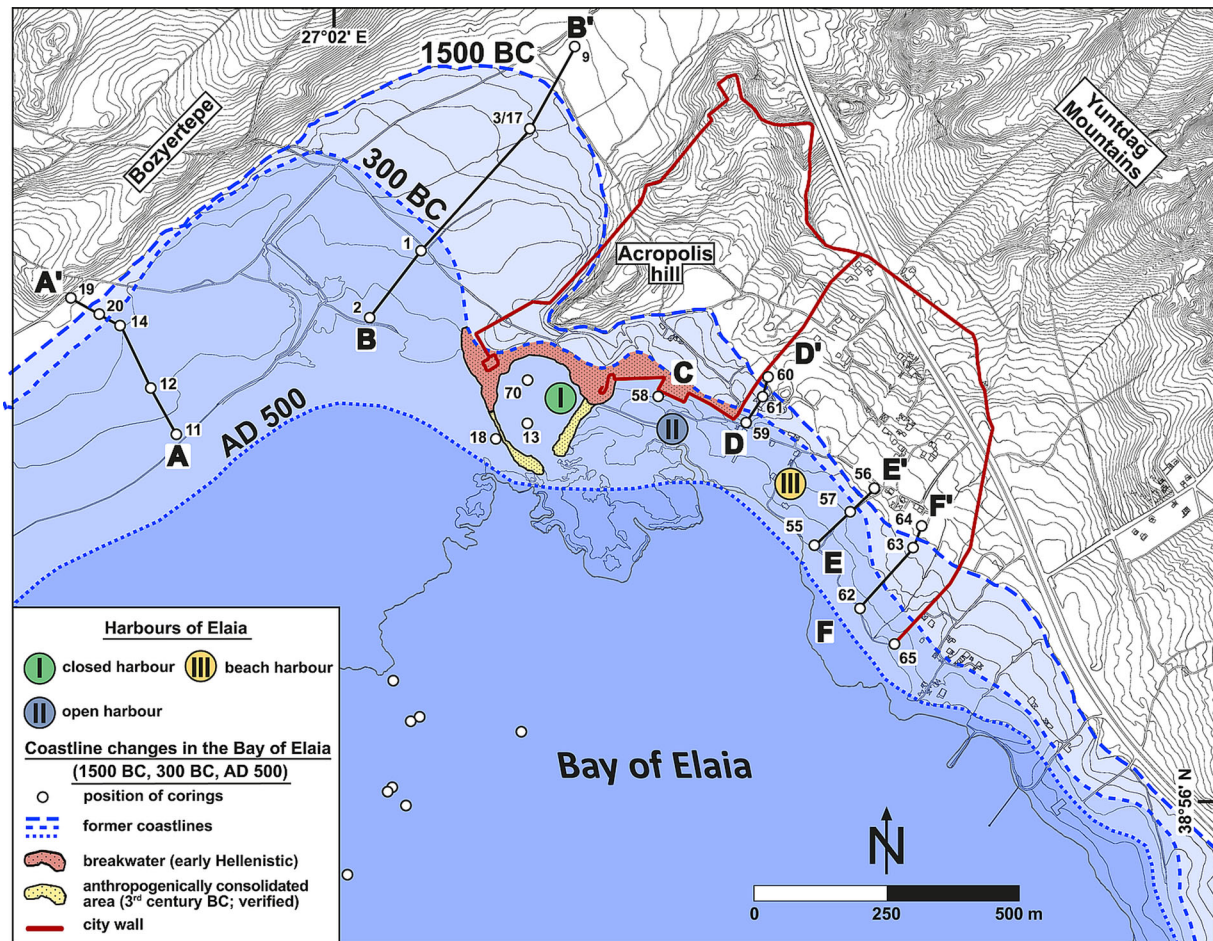The eastern city district experienced a regression of the shoreline caused by terrestrial sediments washed down from

Figure 9. Coastline changes in the Bay of Elaia in time slices: 1500 BC, 300 BC and AD 500. The scenarios are based on the results of this paper.

the nearby slopes and human impacts (Shumilovskikh *et al.*, 2016). The coastal area was ideal for landing battleships while goods were probably processed in the closed and the open harbours (Pirson 2011, 2014; Seeliger *et al.*, 2017). Torrential floods could have been a common but temporary problem in the area, but nothing is known about this from the literature. Further south the shoreline leaves a narrow passage between the slopes of the Yuntdağ and the sea (Figs 1, 2 and 9). This underlines Elaia's strategic position: the city served not only as the main harbour of Pergamon, but also as a defensive stronghold, securing the southern entrance to the inner realm of the lower Kaikos area (Seeliger *et al.*, 2013; Pirson, 2014; Figs 1 and 2). This topographical setting is comparable to that of Thermopylae in central Greece, where, in 480 BC, 300 Spartans withstood the far larger Persian army due to their strategic use of the landscape (Kraft *et al.*, 1987). Furthermore, it is reasonable to assume that a defensive turret fortified the southern end of the city wall (Pirson, 2010). A turret would have necessitated a solid foundation when being constructed in a nearshore position; however, no such foundation was detected by coring. In Ela 65 (Figs 2a and 9) only littoral sediments dating to the late Hellenistic to Roman periods were revealed.

AD 500

This scenario represents the time when Elaia was at or near the end of its prime. In several areas, the shoreline was close to its present position and sea level was only 0.4–0.6 m lower than today (Seeliger *et al.*, 2017). All corings present terrestrial sedimentation patterns for this period. The closed

harbour basin had been abandoned and nearly silted up. The area of the former ship sheds was no longer accessible (Seeliger *et al.*, 2013, 2017). Because the harbours were no longer usable, the city was abandoned. Fearing pirate attacks, they probably moved to the landward settlement of *Püsküllü Tepeler* (Pirson, 2010; Seeliger *et al.*, 2014). As documented by pollen data, the natural vegetation grew back and many areas returned to woodland (Shumilovskikh *et al.*, 2016). Saltworks were constructed, mostly built using spolia, about 2 km south of the city in the shallow bay. Salt was of great economic value and it was easy to harvest using a small workforce. Very shallow marine conditions and a very low-energy wave climate in the bay favoured its use as a saltworks (Pirson, 2014; Seeliger *et al.*, 2014).

Elaia in the broader context of the Turkish Aegean coast

Most ancient settlements in the Turkish Aegean region were situated along the coasts of enlarged marine embayments, formed during the Holocene marine transgression. Around 6000 BP, when sea-level rise slowed (Lambeck, 1996; Lambeck and Purcell, 2007), rivers became prominent morphogenetic agents, governing coastal changes by sediment supply, due to their prograding deltas. These settlements (e.g. Troy, Ainos, Ephesus and Miletos) faced numerous environmental challenges, such as the siltation of their harbours or the loss of their connection to the open sea (for locations see Fig. 1b).

Troy is one of the most famous and best-studied examples (Figs 1b and 10a; Kraft *et al.*, 1980, 2003). At the end of the Holocene marine transgression, the sea penetrated inland,
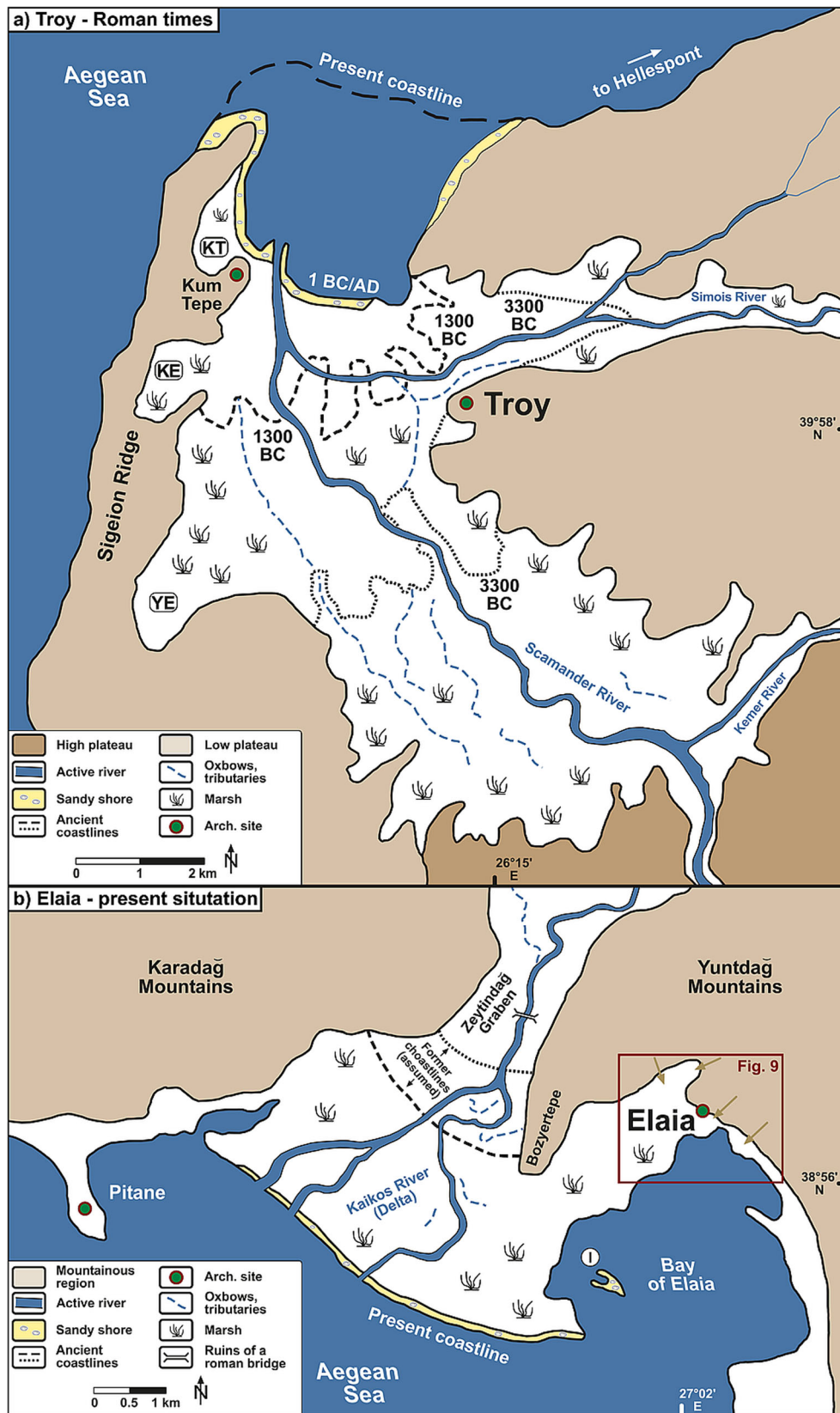
Figure 10. Comparison of the palaeoenvironmental evolution of Troy and Elaia. (a) The area of ancient Troy in Roman times. This clearly shows the influence of the Simois and Scamander Rivers on the areas surrounding Troy, especially with regard to the coastline scenarios for 3300 BC (Late Neolithic/Early Bronze Age), 1300 BC (Iliad/Trojan War) and Roman times (based on Kraft *et al.*, 2003; abbreviations: KT = Kum-Tepe plain, KE = Keşik plain, YE = Yeniköy plain). (b) Present coastline configuration of the Bay of Elaia and the southernmost part of the Kaikos River plus assumed former coastlines of the Kaikos Delta. It is clear that the prograding delta of the Kaikos River did not influence the Bay of Elaia due to the shielding effect of the Bozyertepe ridge (personal compilation based on a QuickBird 2 satellite image, acquired: 2 April 2006).

about 10 km south of the later location of Troy. Deltaic progradation of the Scamander and Simois River followed by floodplain aggradation led to a northward shift of the shoreline. In the early Bronze Age (c. 3300 BC) Troy, as well as the Neolithic settlement of Kumtepe, were seaboard sites – comparable to the scene around 1500 BC in Elaia (Fig. 9) – extending into a shallow marine embayment that still reached some kilometres further south and east of the settlements. At the time of the mythical Trojan War at the end of the late Bronze Age (probably around 1200 BC) the delta front lay beyond but close to the settlement (Kraft et al., 1980, 2003; Hertel, 2008; Brown, 2017). The present shoreline is situated some 4 km north of Troy and a strong longshore drift has hindered further seaward progradation of the delta (Fig. 10a). Due to the long settlement history (3300 BC until AD 1200/1300 with interruptions, Troia I–Troia IX), the city hosted different harbour sites following the migrating shoreline. Based on a detailed summary of published work since the 1980s, Kayan (2014) suggests three possible harbour locations on the eastern slope of the Sigeion ridge (Fig. 10a). However, the southernmost possible location in the Yeniköy plain (YE in Fig. 10a) was already landlocked between 5000 and 3500 BP and a westward connection to the open Aegean by a canal or ditch crossing the Sigeion ridge can be excluded. The silting up history of the Keşik plain (KE in Fig. 10a) remains open to discussion. While Kayan (2014) states that it was a swamp at the time of the Trojan War, Kraft et al. (2003) assume a near-coastal shallow marine embayment in this area. In contrast to the Yeniköy plain, for the Keşik plain ships could be transported to the other side of the Sigeion ridge. It was possible to transport ships from a protected harbour location in this area to the Aegean although the delta front had already prograded beyond this location. Finally, the northernmost area of the Kumtepe plain (KT in Fig. 10a) silted up last, probably in late Hellenistic or early Roman Imperial times. Although Kayan (2014) does not advocate a harbour in this area, it would have been possible to land vessels at this location throughout the settlement period of Troy (Kraft et al., 2003; Hertel, 2008; Kayan, 2014).

The ancient city of Ainos (Fig. 1b) is located close to the river mouth of the Hebros, which today flows into the Aegean via an extensive deltaic floodplain of 180 km², between the Greek city of Alexandroupoli and the Turkish city of Enez. Postglacial sea-level rise created a marine embayment which reached as far as the modern town of İpsala, i.e. 26 km inland. Later, the delta front passed the city just after Roman Imperial times and may have caused a shift in the location of the city's harbours. Today, the city is situated about 2.5 km inland, separated from the Aegean by an extensive beach-barrier system (Alpar, 2001; Anthony et al., 2014; Brückner et al., 2015).

Further south, at ancient Ephesus (Fig. 1b) and its famous Artemision, sediment transported by the Küçük Menderes river led to widespread siltation of the Küçük Menderes graben. The prograding delta caused the harbours to silt up and the Ephesians were eventually forced to construct a 'harbour channel' to maintain an access route to the sea after the delta front prograded beyond the city (e.g. Kraft et al., 2007; Delile et al., 2015; Ledger et al., 2018).

Finally, the palaeoenvironmental model for the Küçük Menderes graben can also be transposed to the Büyük Menderes graben, c. 50 km south. As the longest waterway flowing into the Turkish Aegean, the Büyük Menderes river led to the disconnection of ancient Miletos and Priene, situated on the southern flank of the Büyük Menderes graben, from the open sea and the demise of their harbours (e.g. Brückner et al., 2006, 2013; Kazancı et al., 2009).

In contrast, Fig. 10b shows the coastal configuration of the wider Elaia region. Unlike the above-mentioned settlements, Elaia is not situated on the inner part of the Kaikos or Zeytindağ graben. The Bozyertepe ridge separates it from the Zeytindağ graben and therefore protects it from the fluvial sediments of the Kaikos. This is supported by the absence of fluvial sediments in the cores (unit 6). Siltation of the harbours of Elaia was therefore not as strongly triggered by deltaic progradation as for the above-mentioned examples, but also by slope wash of terrestrial material from the nearby Yuntdağ and Bozyertepe. As studies investigating the deltaic evolution of the Kaikos are lacking, we cannot speculate on this topic. Nevertheless, remains of a Roman-age bridge, just west of the Bozyertepe, documents that the delta front had already prograded beyond this location before this date. Based on corings, the evolution of the small island (I on Fig. 10b) was dated to the post-15th century AD (Körfgen, 2014), showing that the most distal extension of the delta occurred recently. As a result, because the influence of a major river delta is secondary, the harbour basins of Elaia were not massively affected by siltation, as borne out by the absence of dredging. Dredging is widely attested to in other Mediterranean harbours such as Naples (Delile et al., 2016), Portus (Salomon et al., 2012), Tyre (Marriner and Morhange, 2006), Marseille (Morhange et al., 2003) and Ephesus (Kraft et al., 2007; Delile et al., 2015). In addition, due to the short settlement period of Elaia (maximum 1000 years) – bracketed by natural conditions before and after it – the closed harbour basin constitutes a valuable geoarchive (Shumilovskikh et al., 2016).

Conclusions

Around 1500 BC, the marine extension in the Bay of Elaia was at its maximum. The sea extended c. 400 m inland in the northern and western areas; thus, the Acropolis was transformed into a peninsula. Due to the adjacent Yuntdağ the extension of the sea to the east of Elaia was far less significant than in the western part. Siltation led to gradual regression of the shoreline, largely due to human activity over the next few centuries (Shumilovskikh et al., 2016).

During Hellenistic and Roman times, from ~300 BC onwards, three harbour areas were operational: the closed harbour, the open harbour and the beach harbour. While the closed harbour was used for commercial and military purposes, the open harbour probably housed ship sheds with the battleships of the Pergamenians. The eastern city district with its beach harbour served as a place of temporary residence for foreign merchants, sailors and soldiers (Pirson, 2010, 2014; Pint et al., 2015; Seeliger et al., 2017; Feuser et al., 2018). Siltation of the harbours contributed to the decline of the city in late Roman times and its eventual abandonment (after AD 500). Human activity hugely influenced the landscape. Erosional processes became prominent in the densely populated and intensively used eastern part of the Bay of Elaia while such impacts were relatively minor in the western part, far from the settled area. Pint et al. (2015) have demonstrated that siltation of the open harbour area accelerated during the settlement period of Elaia. This may have resulted from the construction of the closed harbour basin and its breakwaters, which impeding the bay's anit-clockwise coastal cell, creating a sediment trap east of the closed harbour directly in front of the open harbour area (Figs 2 and 9).

While the population of Elaia shrank during Late Antiquity, the remaining inhabitants went to great lengths to construct saltworks, which had a strong influence on the environment

and the sea currents in this area. Finally, in contrast to many other ancient settlements on the Turkish Aegean coast, Elaia was not significantly affected by siltation of a major river delta. As a consequence, no indications − either sedimentological or literary − report dredging inside Elaia's different harbours. Due to the relatively short urban period of around 1000 years, Elaia provides the opportunity to study human–nature relations in the Hellenistic–Roman Imperial period, and the abandonment of a late antique city and the subsequent return to natural conditions (Shumilovskikh et al., 2016; Pirson, in press).

Abbreviations.
a.s.l., above sea level; b.s., below the surface; ERT, electrical resistivity tomography; LOI, loss on ignition; OSL, optically stimulated luminescence; RSL, relative sea level; XRF, X-ray fluorescence.

References

Ad-Hoc-AG Boden. 2005. *Bodenkundliche Kartieranleitung*. Schweizerbart: Stuttgart (in German).

Aksu AE, Piper DJW, Konuk T. 1987. Late Quaternary tectonic and sedimentary history of outer Izmir and Candarli bays, western Turkey. *Marine Geology* **76**: 89–104.

Alpar B. 2001. Plio-Quaternary history of the Turkish coastal zone of the Enez-Evros Delta: NE Aegean Sea. *Mediterranean Marine Science* **2**: 95–118.

Altunkaynak Ş, Yılmaz Y. 1998. The Mount Kozak magmatic complex, Western Anatolia. *Journal of Volcanology and Geothermal Research* **85**: 211–231.

Ammerman AJ, Efstratiou N, Ntinou M et al. 2008. Finding the early Neolithic in Aegean Thrace: the use of cores. *Antiquity* **82**: 139–150.

Anthony EJ, Marriner N, Morhange C. 2014. Human influence and the changing geomorphology of Mediterranean deltas and coasts over the last 6000 years: from progradation to destruction phase? *Earth-Science Reviews* **139**: 336–361.

Bartz M, Klasen N, Zander A et al. 2015. Luminescence dating of ephemeral stream deposits around the Palaeolithic site of Ifri n'Ammar (Morocco). *Quaternary Geochronology* **30**: 460–465.

Bartz M, Rixhon G, Kehl M et al. 2017. Unravelling fluvial deposition and pedogenesis in ephemeral stream deposits in the vicinity of the prehistoric rock shelter of Ifri n'Ammar (NE Morocco) during the last 100 ka. *Catena* **152**: 115–134.

Başaran S. 2010. *Ainos (Enez)*. University of İstanbul Press: İstanbul.

Benjamin J, Rovere A, Fontana A et al. 2017. Late Quaternary sea-level changes and early human societies in the central and eastern Mediterranean Basin: an interdisciplinary review. *Quaternary International* **449**: 29–57.

Blott SJ, Pye K. 2001. GRADISTAT: a grain size distribution and statistics package for the analysis of unconsolidated sediments. *Earth Surface Processes and Landforms* **26**: 1237–1248.

Bonaduce G, Ciampo G, Masoli M. 1975. Distribution of Ostracoda in the Adriatic Sea. *Pubblicazioni della Stazione zoologica di Napoli* **40** (Suppl.): 1–304.

Brown J. 2017. *Homeric Sites Around Troy*. Parrot Press: Canberra.

Brückner H. 1994. Das Mittelmeergebiet als Naturraum. In *Das Alte Rom*, Martin J (ed.). Bertelsmann: München; 13–29.

Brückner H, Müllenhoff M, Gehrels R et al. 2006. From archipelago to floodplain − geographical and ecological changes in

Miletus and its environs during the past six millennia (western Anatolia, Turkey). *Zeitschrift für Geomorphologie N.F.* **142** (Suppl.): 63–83.

Brückner H, Schmidts T, Bücherl H et al. 2015. Die Häfen und ufernahen Befestigungen von Ainos − eine Zwischenbilanz. In *Häfen im ersten Millennium ad. Bauliche Konzepte, herrschaftliche und religiöse Einflüsse*, Schmidts T, Vučetić MM (eds). Verlag des Römisch-Germanischen Zentralmuseums: Mainz; 53–76.

Brückner H, Urz R, Seeliger M. 2013. Geomorphological and geoarchaeological evidence for considerable landscape changes at the coasts of western Turkey during the Holocene. *Geopedology and Landscape Development Research Series* **1**: 81–104.

Cartledge P. 2004. *Alexander the Great. The Hunt for a New Past*. Overlook Press: New York.

Cimerman F, Langer MR. 1991. *Mediterranean foraminifera*. Slovenska Akademija Znanosti in Umetnosti, Academia Scientarium et Artium Slovenca: Ljubljana.

Delile H, Blichert-Toft J, Goiran JP et al. 2015. Demise of a harbor: a geochemical chronicle from Ephesus. *Journal of Archaeological Science* **53**: 202–213.

Delile H, Goiran J-P, Blichert-Toft J et al. 2016. A geochemical and sedimentological perspective of the life cycle of Neapolis harbor (Naples, southern Italy). *Quaternary Science Reviews* **150**: 84–97.

Ernst W. 1970. *Geochemical Facies Analysis*. Elsevier: Amsterdam.

Evelpidou N, Karkani A, Kampolis I et al. 2017. Late Holocene shorelines in east Attica (Greece). *Quaternary International* **436**: 1–7.

Feuser S, Pirson F, Seeliger M. 2018. The harbour zones of Elaia − the maritime city of Pergamum. In *Harbours as Objects of Interdisciplinary Research - Archaeology + History + Geosciences*, von Carnap-Bornheim C, Daim F, Ettel P, Warnke U (eds). Verlag des Römisch-Germanischen Zentralmuseums: Mainz; 91–103.

Flaux C, Marriner N, el-Assal M et al. 2017. Late Holocene erosion of the Canopic promontory (Nile Delta, Egypt). *Marine Geology* **385**: 56–67.

Folk RL, Ward WC. 1957. Brazos River bar [Texas]; a study in the significance of grain size parameters. *Journal of Sedimentary Research* **27**: 3–26.

Giaime M, Morhange C, Cau Ontiveros MÁ et al. 2017. In search of Pollentia's southern harbour: geoarchaeological evidence from the Bay of Alcúdia (Mallorca, Spain). *Palaeogeography, Palaeoclimatology, Palaeoecology* **466**: 184–201.

Goodman BN, Reinhardt E, Dey H et al. 2008. Evidence for Holocene marine transgression and shoreline progradation due to barrier development in Iskele, Bay of Izmir, Turkey. *Journal of Coastal Research* **245**: 1269–1280.

Goodman BN, Reinhardt EG, Dey HW et al. 2009. Multi-proxy geoarchaeological study redefines understanding of the paleocoastlines and ancient harbours of Liman Tepe (Iskele, Turkey). *Terra Nova* **21**: 97–104.

Hadler H, Kissas K, Koster B et al. 2013. Multiple Late-Holocene tsunami landfall in the eastern Gulf of Corinth recorded in the palaeotsunami geoarchive at Lechaion, harbour of ancient Corinth (Peloponnese, Greece). *Zeitschrift für Geomorphologie N.F.* **57**: 139–180.

Hansen E. 1971. *The Attalids of Pergamon*. Cornell University Press: Ithaca.

Hertel D. 2008. *Troia − Archäologie Geschichte Mythos*. C. H. Beck: München.

Horejs B. 2012. Çukuriçi Höyük. A Neolithic and Bronze Age settlement in the region of Ephesos. In *The Neolithic in Turkey. New Excavations & New Research*, Özdoğan M, Başgelen N, Kuniholm P (eds). Archaeology and Art Publications: İstanbul; 117–131.

Horejs B, Milić B, Ostmann F et al. 2015. The Aegean in the early 7th millennium BC: maritime networks and colonization. *Journal of World Prehistory* **28**: 289–330. [PubMed: 27453633].

Jeckelmann C. 1996. *Genese lokaler Thermalwasservorkommen in der Region Bergama/W-Türkei − Hydrochemie, Gas- und Isotopenanalysen zur Korrelation tiefer Grundwasserzirkulation und aktiver Tektonik*. PhD thesis, University of Zürich.

Joachim F, Langer M. 2008. *The 80 Most Common Ostracods from the Bay of Fetoveia, Elba Island (Mediterranean Sea)*. University Bonn Press: Bonn.

Kayan I. 1999. Holocene stratigraphy and geomorphological evolution of the Aegean coastal plains of Anatolia. *Quaternary Science Reviews* **18**: 541–548.

Kayan I. 2014. Geoarchaeological Research at Troia and its Environs. In *Troia 1987–2012: Grabungen und Forschungen I – Forschungsgeschichte, Methoden und Landschaft*, Pernicka E, Rose CB, Jablonka P (eds). Verlag Dr. Rudolf-Habelt: Bonn; 694–731.

Kazancı N, Dündar S, Alçiçek MC et al. 2009. Quaternary deposits of the Büyük Menderes Graben in western Anatolia, Turkey: implications for river capture and the longest Holocene estuary in the Aegean Sea. *Marine Geology* **264**: 165–176.

Khan NS, Ashe E, Shaw TA et al. 2015. Holocene relative sea-level changes from near-, intermediate-, and far-field locations. *Current Climate Change Reports* **1**: 247–262.

Körfgen K. 2014. *Die Analyse des Bohrkerns ELA 84–Ein Beitrag zur sedimentologischen Entwicklung der Bucht von Elaia, Westtürkei*. Bachelor's thesis, University of Cologne.

Kraft JC, Rapp G, Kayan I et al. 2003. Harbor areas at ancient Troy: sedimentology and geomorphology complement Homer's Iliad. *Geology* **31**: 163–166.

Kraft JC, Aschenbrenner SE, Rapp G, Jr. 1977. Paleogeographic reconstructions of coastal Aegean archaeological sites. *Science* **195**: 941–947. [PubMed: 17735653].

Kraft JC, Brückner H, Kayan I et al. 2007. The geographies of ancient Ephesus and the Artemision in Anatolia. *Geoarchaeology* **22**: 121–149.

Kraft JC, Kayan I, Erol O. 1980. Geomorphic reconstructions in the environs of ancient Troy. *Science* **209**: 776–782. [PubMed: 17753292].

Kraft JC, Rapp G, Szemler GJ et al. 1987. The pass at Thermopylae, Greece. *Journal of Field Archaeology* **14**: 181–198.

Lambeck K. 1996. Sea-level change and shore-line evolution in Aegean Greece since Upper Palaeolithic time. *Antiquity* **70**: 588–611.

Lambeck K, Purcell A. 2007. Palaeogeographic reconstructions of the Aegean for the past 20, 000 years: was Atlantis on Athens doorstep? In *The Atlantis Hypothesis: Searching for a Lost Land*, Papamarinopoulos SP (ed). Heliotopos Publications: Santorini; 241–257.

Ledger ML, Stock F, Schwaiger H et al. 2018. Intestinal parasites from public and private latrines and the harbour canal in Roman Period Ephesus, Turkey (1st c. BCE to 6th c. CE). *Journal of Archaeological Science: Reports* **21**: 289–297.

Lubos C, Dreibrodt S, Bahr A. 2016. Analysing spatio-temporal patterns of archaeological soils and sediments by comparing pXRF and different ICP-OES extraction methods. *Journal of Archaeological Science: Reports* **9**: 44–53.

Marriner N, Morhange C. 2006. Geoarchaeological evidence for dredging in Tyre's ancient harbour, Levant. *Quaternary Research* **65**: 164–171.

Marriner N, Morhange C, Kaniewski D et al. 2014. Ancient harbour infrastructure in the Levant: tracking the birth and rise of new forms of anthropogenic pressure. *Scientific Reports* **4**: 5554. [PubMed: 24989979]

Meriç E, Avşar N, Bergin F. 2004. Benthic foraminifera of eastern Aegean Sea (Turkey); systematics and autecology. *Turkish Marine Research Foundation* **18**: 1–306.

Morhange C, Blanc F, Schmitt-Mercury S et al. 2003. Stratigraphy of late-Holocene deposits of the ancient harbour of Marseilles, southern France. *The Holocene* **13**: 593–604.

Morhange C, Giaime M, Marriner N et al. 2016. Geoarchaeological evolution of Tel Akko's ancient harbour (Israel). *Journal of Archaeological Science: Reports* **7**: 71–81.

Murray JW. 2006. *Ecology and Applications of Benthic Foraminifera*. Cambridge University Press: New York.

Murray-Wallace CV, Woodroffe CD. 2014. *Quaternary Sea-Level Changes: A Global Perspective*. Cambridge University Press: Cambridge.

Özbek O. 2010. Hamaylıtarla Reconsidered: a Neolithic site and its environmental setting in southern Turkey. *Anatolia Antiqua* **18**: 1–21.

Pennington BT, Sturt F, Wilson P et al. 2017. The fluvial evolution of the Holocene Nile Delta. *Quaternary Science Reviews* **170**: 212–231.

Pint A, Seeliger M, Frenzel P et al. 2015. The environs of Elaia's ancient open harbour – a reconstruction based on microfaunal evidence. *Journal of Archaeological Science* **54**: 340–355.

Pirson F. 2004. Elaia, der maritime Satellit Pergamons. *Istanbuler Mitteilungen* **54**: 197–213.

Pirson F. 2007. Elaia. *Archäologischer Anzeiger* **2**: 47–58.

Pirson F. 2008. Das Territorium der hellenistischen Residenzstadt Pergamon – Herrschaftlicher Anspruch als raumbezogene Strategie. In *Räume der Stadt - Von der Antike bis heute*, Jöchner C (ed). Reimer: Berlin; 27–50.

Pirson F. 2010. Survey. *Archäologischer Anzeiger* **2**: 195–201.

Pirson F. 2011. Elaia. *Archäologischer Anzeiger* **2**: 166–174.

Pirson F. 2014. Elaia, der (maritime) Satellit Pergamons. In *Harbour Cities in the Eastern Mediterranean from Antiquity to the Byzantine Period*, Ladstätter S, Pirson F, Schmidts T (eds). EgeYayinlari: Istanbul; 339–356.

Pirson F. in press. Nature, religion, and urban aesthetics in Ancient Pergamon and its micro-region. Some thoughts on the potential of an 'ecological turn' for classical archaeology (and beyond) In *Ecologies, Aesthetics, and Histories of Art*, Baader H, Ray S, Wolf G, (eds). de Gruyter: Berlin.

Pirson F. Scholl A. 2015. *Pergamon. A Hellenistic Capital in Anatolia*. Ege Yayinlari: İstanbul.

Radt W. 2016. *Pergamon – Geschichte und Bauten einer antiken Metropole*. Primus Verlag: Darmstadt.

Reimer PJ, Bard E, Bayliss A et al. 2013. IntCal13 and Marine13 radiocarbon age calibration curves 0–50000 years calBP. *Radiocarbon* **55**: 1869–1887.

Salomon F, Delile H, Goiran J-P et al. 2012. The Canale di Comunicazione Traverso in Portus: the Roman sea harbour under river influence (Tiber Delta, Italy). *Géomorphologie* **18**: 75–90.

Seeliger M, Bartz M, Erkul E et al. 2013. Taken from the sea, reclaimed by the sea: the fate of the closed harbour of Elaia, the maritime satellite city of Pergamum (Turkey). *Quaternary International* **312**: 70–83.

Seeliger M, Brill D, Feuser S et al. 2014. The purpose and age of underwater walls in the Bay of Elaia of western Turkey: a multidisciplinary approach. *Geoarchaeology* **29**: 138–155.

Seeliger M, Pint A, Frenzel P et al. 2017. Foraminifera as markers of Holocene sea-level fluctuations and water depths of ancient harbours – A case study from the Bay of Elaia (W Turkey). *Palaeogeography, Palaeoclimatology, Palaeoecology* **482**: 17–29.

Seeliger M, Pint A, Frenzel P et al. 2018. Using a Multi-Proxy Approach to Detect and Date a Buried part of the Hellenistic City Wall of Ainos (NW Turkey). *Geosciences* **8**: 357.

Shumilovskikh LS, Seeliger M, Feuser S et al. 2016. The harbour of Elaia: A palynological archive for human environmental interactions during the last 7500 years. *Quaternary Science Reviews* **149**: 167–187.

Siani G, Paterne M, Arnold M et al. 2000. Radiocarbon reservoir ages in the Mediterranean Sea and Black Sea. *Radiocarbon* **42**: 271–280.

Stock F, Ehlers L, Horejs B et al. 2015. Neolithic settlement sites in Western Turkey – palaeogeographic studies at Çukuriçi Höyük and Arvalya Höyük. *Journal of Archaeological Science: Reports* **4**: 565–577.

Strabo. 2005. *Geographica. Translation and comments by Albert Forbiger*. Marix Verlag: Wiesbaden.

Vacchi M, De Falco G, Simeone S et al. 2016b. Biogeomorphology of the Mediterranean *Posidonia oceanica* seagrass meadows. *Earth Surface Processes and Landforms* **42**: 42–54.

Vacchi M, Marriner N, Morhange C et al. 2016a. Multiproxy assessment of Holocene relative sea-level changes in the western

Mediterranean: sea-level variability and improvements in the definition of the isostatic signal. *Earth-Science Reviews* **155**: 172–197.

Vacchi M, Rovere A, Chatzipetros A et al. 2014. An updated database of Holocene relative sea level changes in NE Aegean Sea. *Quaternary International* **328–329**: 301–310.

Vita-Finzi C. 1969. Late Quaternary continental deposits of central and western Turkey. *Man New Series* **4**: 605–619.

Vött A, Bareth G, Brückner H et al. 2011. Olympia's harbour site Pheia (Elis, Western Peloponnese, Greece) destroyed by tsunami impact. *Erde* **142**: 259–288.

Yoo J, Rohli RV. 2016. Global distribution of Köppen–Geiger climate types during the Last Glacial Maximum, Mid-Holocene, and present. *Palaeogeography, Palaeoclimatology, Palaeoecology* **446**: 326–337.